Ceramics-Silikáty 61 (1), 1-5 (2017)
journal webpage: www.ceramics-silikaty.cz doi: 10.13168/cs.2016.0052

PHASE EVOLUTION AND MICROWAVE DIELECTRIC PROPERTIES OF $Ca_{0.61}Nd_{0.26}Ti_{1-x}(Al_{1/2}Nb_{1/2})_xO_3$ CERAMICS ($0 \leq x \leq 0.2$)

HETUO CHEN*, **, #BIN TANG*, **, PENG FAN**, MENG WEI**, SHUREN ZHANG*, **

*National Engineering Research Center of Electromagnetic Radiation Control Materials,
University of Electronic Science and Technology of China, Jianshe Road, Chengdu 610054, People's Republic of China
**State Key Laboratory of Electronic Thin Films and Integrated Devices,
University of Electronic Science and Technology of China, Jianshe Road, Chengdu 610054, People's Republic of China

#E-mail: tangbin@uestc.edu.cn

Submitted May 23, 2016; accepted September 17, 2016

Keywords: Microwave dielectric properties, Substitution, $Ca_{0.61}Nd_{0.26}TiO_3$

Phase evolution and microwave dielectric properties of $Ca_{0.61}Nd_{0.26}Ti_{1-x}(Al_{1/2}Nb_{1/2})_xO_3$ ceramics in the range of $0 \leq x \leq 0.2$ have been determined in this paper. For $0 \leq x \leq 0.1$, X-ray diffraction results showed a single perovskite structure phase. Dielectric constant (ε_r) and quality factor ($Q \times f$) kept high values and temperature coefficient of resonant frequency (τ_f) decreased by 32.4 % from 247 ppm/°C to 167 ppm/°C. When $0.15 \leq x \leq 0.2$, extra peaks with peak positions coincidental with $Ca_2Nb_2O_7$ phase appeared. Typically, high relative permittivity (≥ 90) and quality factor (≥ 6,400 GHz) could be obtained when sintered at 1400°C for 2 h.

INTRODUCTION

Microwave dielectric ceramics have been widely utilized in wireless communication systems [1], such as RFID devices [2, 3], Radar [1], and mobile telephone [1]. Microwave dielectric materials in these applications are guided by the high relative permittivity to minimize the device size [2, 3], the high Q value to optimize the signal selection, and near zero temperature coefficients at resonant frequency for a stable work frequency[1]. This guidance gives rise to wide researches on high dielectric constant ceramics for their impractical τ_f values.

The high dielectric constant ceramics of $CaTiO_3$ [4], BaO-Nd_2O_3-TiO_2 [5], and Bi_2O_3-V_2O_5 [6] are intensively reported and $CaTiO_3$ shows the highest relative permittivity. Until now, many reports on the ionic substitution in $CaTiO_3$ have been proved as an effective way modifying the temperature coefficient at the resonant frequency to zero. To name a few, $CaTi_{0.1}(Li_{1/3}Nb_{2/3})_{0.9}O_3$ [7], $CaTi_{0.54}(Al_{1/2}Ta_{1/2})_{0.46}O_3$ [8], $CaTi_{0.5}(Al_{1/2}Nb_{1/2})_{0.5}O_3$ [9], $CaTi_{0.34}(Mg_{1/3}Nb_{2/3})_{0.66}O_3$ [10, 11], all exhibit high quality factor and near zero τ_f value. One interesting fact is that, though $Ca(Al_{1/2}Nb_{1/2})O_3$ shows relative low quality factor (7500 GHz)[4], $(Al_{1/2}Nb_{1/2})^{4+}$ substituted $CaTiO_3$ possesses rather high quality factor (> 20000 GHz) [9]. Also, this substitution study in $Ca_{0.61}Nd_{0.26}TiO_3$, originating from $CaTiO_3$ and exhibiting microwave dielectric properties of $\varepsilon_r \sim 100$, $Q \times f \sim 8600$ GHz and $\tau_f \sim +250$ ppm/°C [12], has not been reported yet. So it would be necessary to clarify the phase evolution and microwave dielectric properties of the $(Al_{1/2}Nb_{1/2})^{4+}$ substituted $Ca_{0.61}Nd_{0.26}TiO_3$ ceramic.

In the present work, $Ca_{0.61}Nd_{0.26}Ti_{1-x}(Al_{1/2}Nb_{1/2})_xO_3$ ($0 \leq x \leq 0.2$) ceramic were fabricated according to the conventional solid state reaction method. The solid solution limit was determined and the corresponding microwave dielectric properties were also investigated.

EXPERIMENTAL

By the conventional solid-state reaction routine, samples were prepared according to $Ca_{0.61}Nd_{0.26}Ti_{1-x}(Al_{1/2}Nb_{1/2})_xO_3$ ($0 \leq x \leq 0.2$) with $CaCO_3$ (Xilong Group, China), Nd_2O_3 (Jichang Rare Earth Co., Ltd China), TiO_2 (Xian Tao Chemical Reagent Co., Ltd., China), Al_2O_3 (Betterwear New Matrial Co., Ltd., China) and Nb_2O_5 (Ke Long Chemical Reagent Co., Ltd., China), as starting materials, with purity ≥ 99.5 %. The mixtures were ball-milled in nylon jars with zirconia balls and deionized water for 8 hours (1:5:1.5). After the drying procedure (120°C for 24 hours), the powders were sifted and calcined at 1150°C for 5 hours. Then the calcined powders were produced with 6 wt. % PVA in the size of 14.5 mm in diameter and 7 mm in thickness under the pressure of 250 kg·cm^{-2} with a stainless steel die [12]. Then the samples were preheated at 600°C for 2 hours to remove the organic binder and then sintered at 1350 - 1425°C for 2 hours.

Densities of sintered samples were measured by the Archimedes method. The phases of the sintered samples were identified by the X-ray diffraction (XRD) using the Cu K alpha radiation (40 kV/250 mA, wavelength = 1.54062 Å, Philips x'pert Pro MPD, PANalytical, the Netherlands). Lattice parameters were calculated by the Unitcell using the Rietveld analysis. XRD results refinement were established by the Maud. The surface microstructures of the ceramic were detected by the scanning electron microscopy (SEM, FEI Inspect F). The dielectric characteristics were examined by the Hakki-Coleman dielectric resonator method in the TE_{011} mode using a network analyzer (Agilent Technologies E5071C, Agilent Technologies, Singapore) at the frequency around 3 - 5 GHz. The τ_f values of sintered samples at the resonant frequency were determined by the equation as following:

$$\tau_f = \frac{f_{t2} - f_{t1}}{f_{t1} \times (t_2 - t_1)} \times 10^6 \quad (1)$$

In the equation, f_{t1} and f_{t2} are the resonant frequencies at the temperature of t_1 (ordinary temperature) and t_2 = 85°C respectively.

RESULTS AND DISCUSSION

Figure 1 showed the X-ray diffraction patterns of $Ca_{0.61}Nd_{0.26}Ti_{1-x}(Al_{1/2}Nb_{1/2})_xO_3$ ($0 \le x \le 0.2$) ceramics sintered at optimum temperature for 2 h. For $0 \le x \le 0.1$, it kept a single perovskite structure phase (JCPDS Card No. 01-082-0229). The single phase probably was because of the two reasons: relative low content of Al_2O_3/Nb_2O_5 addition or the formation of the solid solution. For there was no extra peak, we excluded the first situation. For the second situation, there will be lattice parameter change. In order to prove this, we compared the measured and calculated XRD results, as shown in Figure 2. The discrepancy between observed and calculated data was small, with some deviation at main peaks [13]. The corresponding lattice parameters were also calculated according to the XRD data and the results were depicted in Figure 3. Parameters of three axes and unit cell volume showed a dropping trend. This is reasonable because of similar ionic radius of Ti^{4+} (0.0605 nm) and $(Al_{1/2}Nb_{1/2})^{4+}$ (0.0588 nm), and we concluded that the solid solution of perovskite structure was formed. For $0.15 \le x \le 0.2$, extra peaks appeared, which were coincidental with the $Ca_2Nb_2O_7$[14] (JCPDS Card No. 00-042-0002) phase, and no other extra phase peaks were detected. The appearance of the secondary phase determined that the solid solution limit was around 0.1.

Microstructure images of $Ca_{0.61}Nd_{0.26}Ti_{1-x}(Al_{1/2}Nb_{1/2})_xO_3$ ($0 \le x \le 0.2$) ceramics sintered at 1400°C were shown in Figure 4a-e. As x value growing from 0 to 0.1 the grain size dropped rapidly from around 100 μm to 25 μm while the number of pores located at the edge of the grains grew up quickly. After that, the grain size was stable at about

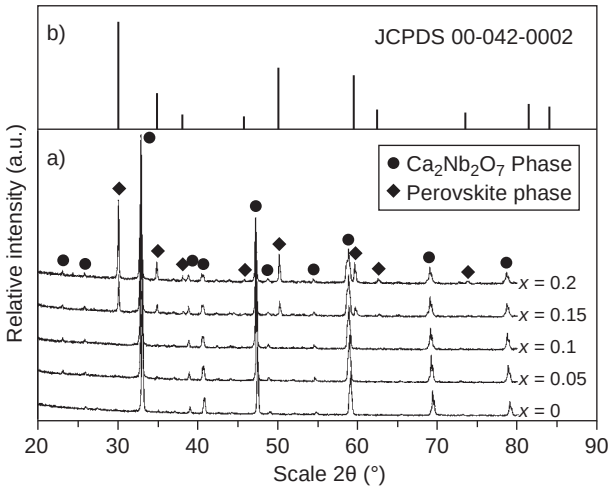

Figure 1. The XRD patterns of $Ca_{0.61}Nd_{0.26}Ti_{1-x}(Al_{1/2}Nb_{1/2})_xO_3$ ($0 \le x \le 0.2$) ceramics sintered at 1400°C for 2 h.

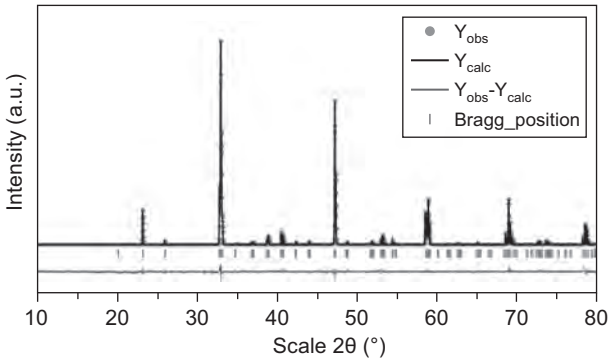

Figure 2. Experimental (Red) and calculated (Black) X-ray powder diffraction profiles for $Ca_{0.61}Nd_{0.26}Ti_{1-x}(Al_{1/2}Nb_{1/2})_xO_3$, x = 0.05, 1400°C for 2 h, R = 12 %.

Table 1. Microwave dielectric properties and tolerance factor of $Ca_{0.61}Nd_{0.26}[Ti_{1-x}(Al_{1/2}Nb_{1/2})_x]O_3$ ($0 \le x \le 0.2$) ceramics sintered at 1400°C for 2h.

x	Sintering temperature (°C)	Relative density	ε_r	$Q \times f$ (GHz)	τ_f (ppm/°C)	Tolerance factor
0	1400	97 %	103	8600	+247	0.8487
0.05	1400	96.6 %	101.6	7880	+213	0.8495
0.1	1400	95.7 %	92.3	6420	+167	0.85024
0.15	1400	–	87.4	4200	+134	–
0.2	1400	–	78.5	3200	+104	–

20 μm and the pore number stayed as well. However, though we've observed peaks of $Ca_2Nb_2O_7$ phase, it was hard to figure out them in the SEM images. This was probably due to their similar appearance.

The apparent densities of the specimens were measured by the Archimedes method and depicted in Figure 5. For each composition at different sintering temperature, it showed a growing trend when temperature grew from 1350°C to 1400°C and then a declination, which inferred 1400°C was the optimal sintering temperature. As x value increasing from 0 to 0.2, the density of sintered ceramic kept decreasing which were consistent with the SEM results. Its trend was the same as pore number variation for $x \sim 0$ to 0.1.

Microwave dielectric properties of optimal temperature sintered $Ca_{0.61}Nd_{0.26}Ti_{1-x}(Al_{1/2}Nb_{1/2})_xO_3$ ($0 \le x \le 0.2$) ceramics were listed in Table 1. The dielectric constant versus x value dropped from 103 to 78.5. The quality factor and temperature coefficient of resonant frequency both declined as well. For $0 \le x \le 0.1$, though the grain size decreased tremendously, relative density of specimens were higher than 95 %, we concluded that the dielectric constant was controlled by average ionic polarizability, which has been clarified in [2, 15, 16]. For the decreasing quality factor, it probably was because of the decreasing grain size, in other words more grain boundaries in unit volume [17]. The grain boundary could act as a two-dimension defect interrupting the symmetry of the crystal, thus smaller grain size, in other words, more defects, will give rise to lower $Q \times f$ [10]. Also, the increment of electrons (Nb^{5+} donor doping), resulting from high content doping: $Nb_2O_5 \xrightarrow{TiO_2} 2Nb_{Ti}^{\cdot} + 4O_o^x + \frac{1}{2}O_2 + \uparrow 2e$ [18, 20] was another factor causing the decrease of $Q \times f$. It has been reported that dielectric loss was proportional to conductivity, tan δ σ, so that too much substitution would lead to low Q value [18, 20]. The substitution at Ti^{4+} site slightly changed lattice parameters that influenced the degree of tilting of octahedral [10]. And tolerance factor was always calculated to measure the degree which was always reported to influence the τ_f value [10]. Consequently, the tolerance factor was calculated by the following equation [21] and the data were in Table 1:

$$t = \frac{0.61R_{Ca^{2+}} + 0.26R_{Nd^{3+}} + R_{O^{2-}}}{\sqrt{2}[(1-x)R_{Ti^{4+}} + \frac{x}{2}R_{Al^{3+}} + \frac{x}{2}R_{Nb^{5+}} + R_{O^{2-}}]} \quad (2)$$

With increasing substitution content, tolerance factor inferred a decreasing temperature coefficient of resonant frequency. For $0.15 \le x \le 0.2$, the reason for the drop of microwave dielectric properties was probably due to the secondary phase, with ε_r = 33.6, $Q \times f$ = 1300 GHz and τ_f = -103 ppm/°C [14].

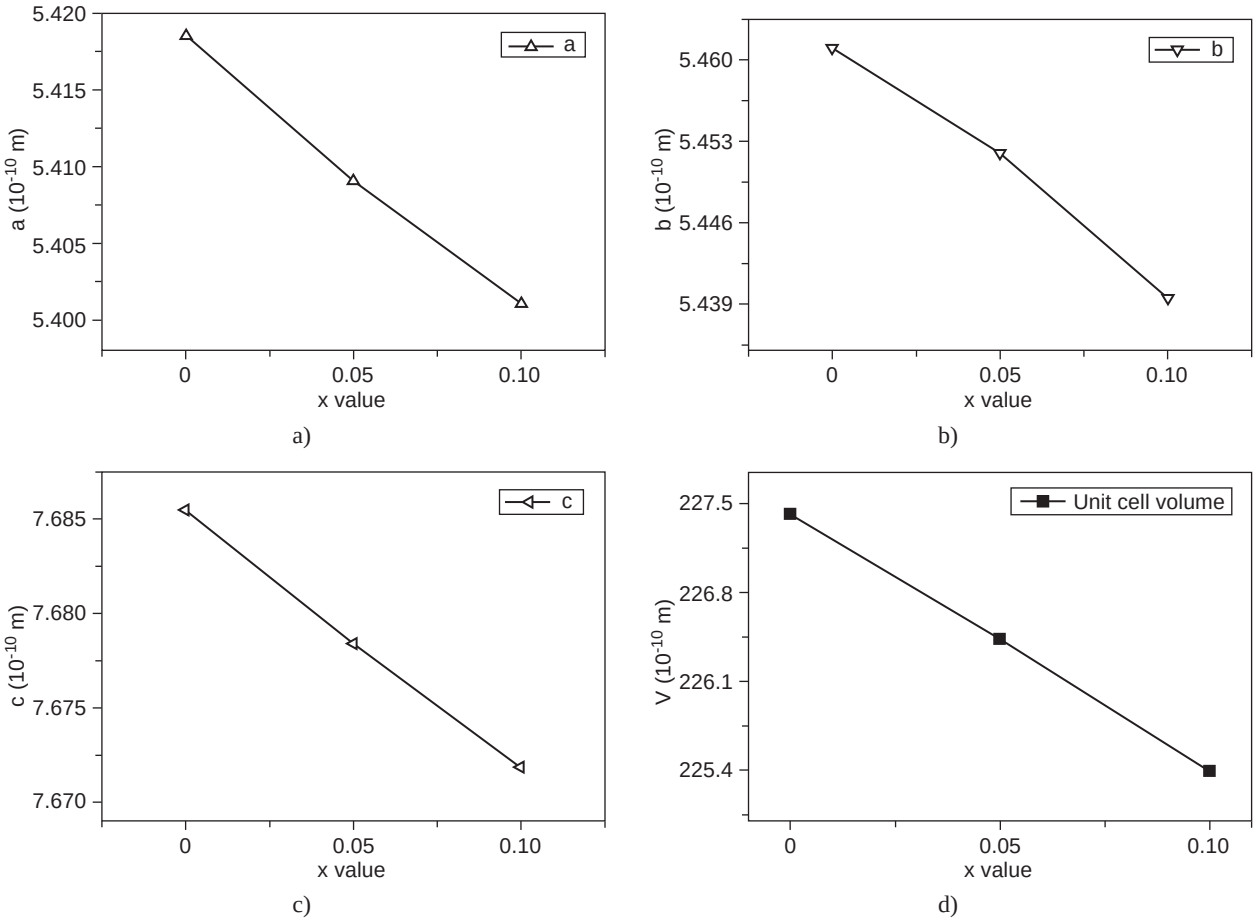

Figure 3. Lattice parameters of $Ca_{0.61}Nd_{0.26}Ti_{1-x}(Al_{1/2}Nb_{1/2})_xO_3$ ($0 \le x \le 0.1$) ceramics as a function of x value.

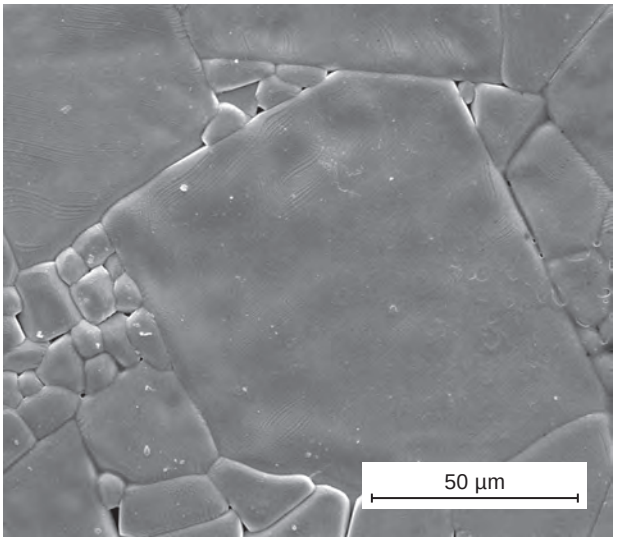

a)

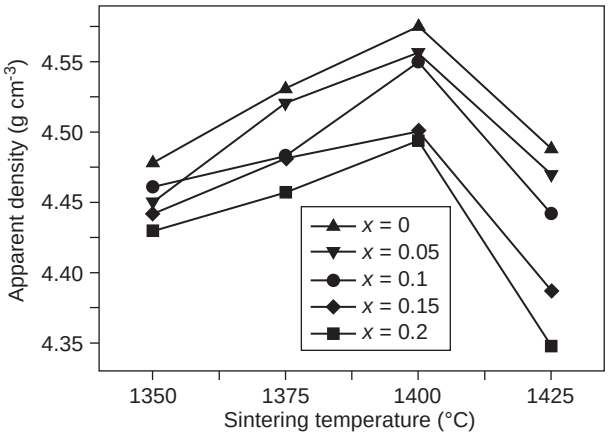

Figure 5. Apparent densities of $Ca_{0.61}Nd_{0.26}Ti_{1-x}(Al_{1/2}Nb_{1/2})_xO_3$ ($0 \leq x \leq 0.2$) ceramics sintered at different temperatures for 2 hours.

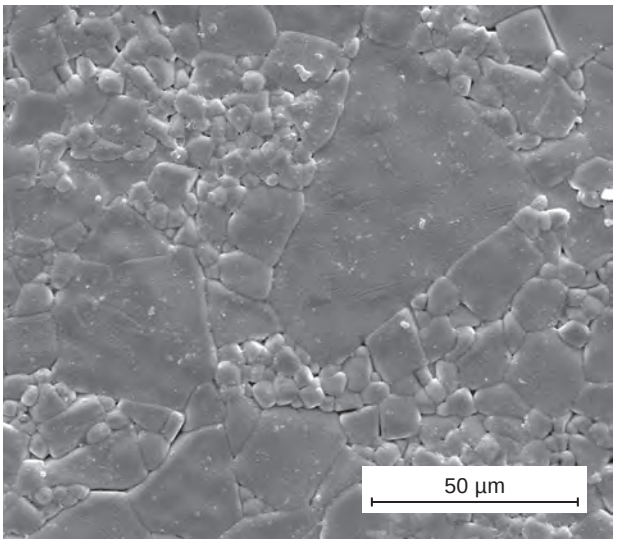

b)

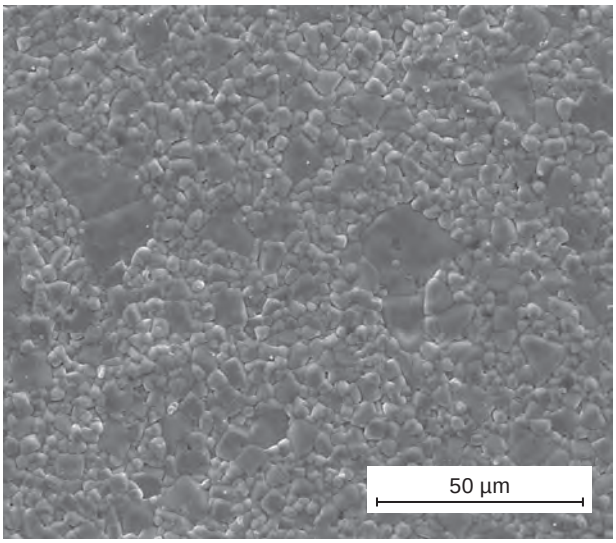

d)

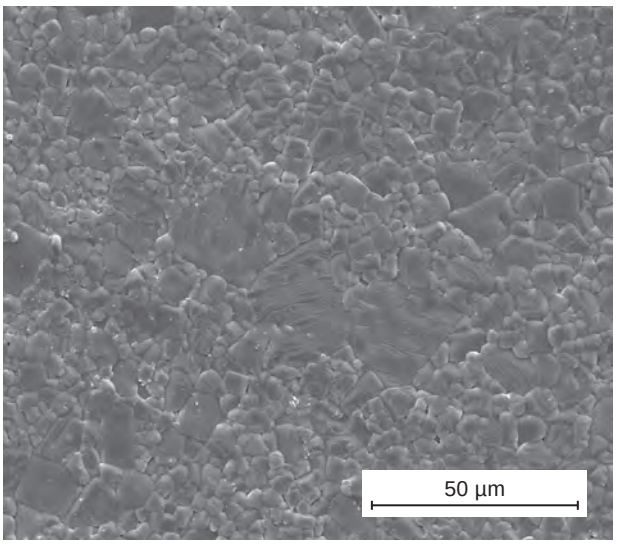

c)

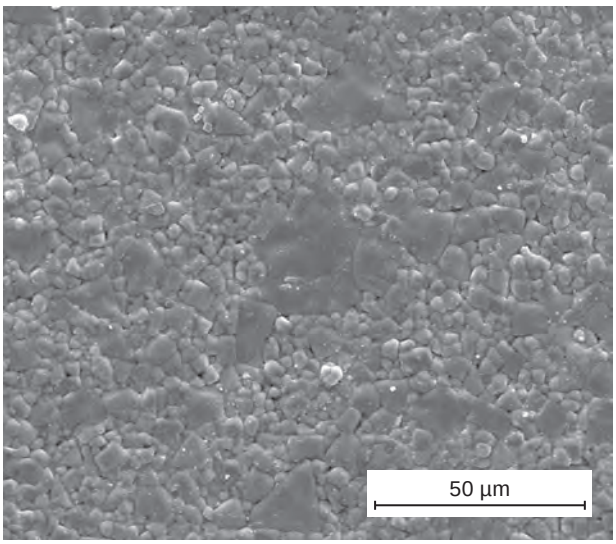

e)

Figure 4. SEM images of $Ca_{0.61}Nd_{0.26}Ti_{1-x}(Al_{1/2}Nb_{1/2})xO_3$ ($0 \leq x \leq 0.2$) ceramics sintered at 1400°C for 2 h: a) $x = 0$, 50 μm, b) $x = 0.05$, 50 μm, c) $x = 0.1$, 50 μm, d) $x = 0.15$, 50 μm, e) $x = 0.2$, 50 μm.

CONCLUSION

Phase evolution and microwave dielectric properties of $Ca_{0.61}Nd_{0.26}Ti_{1-x}(Al_{1/2}Nb_{1/2})_xO_3$ ($0 \le x \le 0.2$) system have been investigated in the study. A single perovskite structure phase was kept for $0 \le x \le 0.1$ and then $Ca_2Nb_2O_7$ secondary phase appeared. The substitution largely changed the microstructure, which was related to relative density and pore ratio determining relative permittivity and $Q \times f$ value of the system. Tolerance factor was calculated to evaluate the τ_f value declination. After exceeding the solid solution, the properties of the secondary phase dominated the property change of the system. At last, within solid solution limit, dielectric constant higher than 92, $Q \times f$ higher than 6400 GHz while partially tailored τ_f value around 160 ppm/°C could be obtained, which gives a new method to modify properties of $CaTiO_3$ ceramics.

Acknowledgments

This work is supported by the Open Foundation of National Engineering Research Center of Electromagnetic Radiation Control Materials (ZYGX2014K003-6) and it is also supported by the National Natural Science Foundation of China (Grant No. 51402039).

REFERENCES

1. Sebastian M.T. (2008). *Dielectric materials for wireless communication*. 1st ed. Elsevier, UK Oxford.
2. Chen H., Tang B., Duan S., Yang H., Li Y., Li H., Zhang S. (2015): Microstructure and Microwave Dielectric Properties of $Ba_{3.75}Nd_{9.5}Ti_{18-z}(Mg_{1/3}Nb_{2/3})_zO_{54}$ Ceramics. *Journal of Electronic Materials*, *44*(4), 1081-1087. doi:10.1007/s11664-015-3630-y
3. Hsu C. H., Huan, C.J. (2014): Preparation, structural and microwave dielectric properties of $CaLa_4(Zr_xTi_{1-x})_4O_{15}$ ceramics. *Journal of Alloys and Compounds*, *587*, 45-49. doi:10.1016/j.jallcom.2013.10.168
4. Cockayne E. (2001): Comparative dielectric response in $CaTiO_3$ and $CaAl_{1/2}Nb_{1/2}O_3$ from first principles. *Journal of Applied Physics*, *90*(3), 1459-1468. doi:10.1063/1.1380991
5. Chen H., Tang B., Xiong Z., Li Y., Zhang S. (2015): Microwave dielectric properties of bismuth-substituted $Ba_{3.75}Nd_{9.5}Ti_{17}Al_{4/3}O_{54}$ ceramics. *Applied Physics A*, *121*(1), 283-287. doi:10.1007/s00339-015-9431-6
6. Zhou D., Guo D., Li W.B., Pang L.X., Yao X., Wang D.W., Reaney I.M. (2016): Novel temperature stable high-ε_r microwave dielectrics in the Bi_2O_3-TiO_2-V_2O system. *Journal of Materials Chemistry C*, *4*(23), 5357-5362. doi:10.1039/C6TC01431C
7. Costa A.B., Sousa D.G., Costa R.C.S., de O Amarante F.W., Fernandes T.S.M., Saraiva G.D., Silva M.A.S., Sombra A.S.B. (2011): High thermal stability of the microwave dielectric properties of $CaTi_{1-x}(Nb_{2/3}Li_{1/3})_xO_{3-\delta}$ alloys, *Physica Scripta*, *84*(5), 055701. doi:10.1088/0031-8949/84/05/055701
8. Kucheiko S., Choi J. W., Kim H.J., Jung H.J. (1996): Microwave Dielectric Properties of $CaTiO_3$-$Ca(Al_{1/2}Ta_{1/2})O_3$ Ceramics. *Journal of the American Ceramic Society*, *79*(10), 2739-2743. doi:10.1111/j.1151-2916.1996.tb09040.x
9. Kucheiko S., Yeo D.H., Choi J.W., Yoon S.J., Kim H.J. (2002): Microwave Dielectric Properties of $CaTiO_3$-$CaAl_{1/2}Nb_{1/2}O_3$ ceramics doped with Li_3NbO_4. *Journal of the American Ceramic Society*, *85*(5), 1327-1329. doi:10.1111/j.1151-2916.2002.tb00272.x
10. Zhao F., Yue Z.X., Zhang Y.C., Gui Z.L., Li L.G. (2005): Microstructure and microwave dielectric properties of $Ca[Ti_{1-x}(Mg_{1/3}Nb_{2/3})_x]O_3$ ceramics, *Journal of the European Ceramic Society*, *25*(14), 3347-3352. doi:10.1016/j.jeurceramsoc.2004.07.036
11. Huang C.L., Chen H.L., Wu C.C. (2001): Improved high Q value of $CaTiO_3$-$Ca(Mg_{1/3}Nb_{2/3})O_3$ solid solution with near zero temperature coefficient of resonant frequency. *Materials Research Bulletin*, *36*(9), 1645-1652. doi:10.1016/S0025-5408(01)00652-3
12. Chen H.L., Huang C.L. (2002): Microwave dielectric properties and microstructures of $Ca_{1-x}Nd_{2x/3}TiO_3$-$Li_{1/2}Nd_{1/2}TiO_3$ ceramics. *Japanese Journal of Applied Physics, 41(9R),* 5650. doi:10.1143/JJAP.41.5650
13. Jankovsky O., Sofer Z., Vitek J., Simek P., Ruzicka K., Svoboda P., Sedmidubsky D. (2015): Structure, oxygen non-stoichiometry and thermal properties of $(Bi_{0.4}Sr_{0.6})Sr_2CoO_{5-\delta}$. *Thermochimica Acta*, *600*, 89-94. doi:10.1016/j.tca.2014.12.002
14. Li C., Wei X., Yan H., Reece M.J. (2012): Microwave dielectric properties of $La_3Ti_2TaO_{11}$ ceramics with perovskite-like layered structure. *Journal of the European Ceramic Society*, *32*(16), 4015-4020. doi:10.1016/j.jeurceramsoc.2012.06.002
15. Chen G.H., Xu H.R., Yuan C.L. (2013): Microstructure and microwave dielectric properties of $Li_2Ti_{1-x}(Zn_{1/3}Nb_{2/x})_xO_3$ ceramics. *Ceramics International*, *39*(5), 4887-4892. doi:10.1016/j.ceramint.2012.11.081
16. Shannon R.D. (1993): Dielectric polarizabilities of ions in oxides and fluorides. *Journal of Applied Physics*, *73*(1), 348-366. doi:10.1063/1.353856
17. Roopas Kiran S., Sreenivasulu G., Murthy V.R.K., Subramanian V., Murty B.S. (2012): Effect of Grain Size on the Microwave Dielectric Characteristics of High-Energy Ball-Milled Zinc Magnesium Titanate Ceramics. *Journal of the American Ceramic Society*, *95*(6), 1973-1979. doi:10.1111/j.1551-2916.2012.05128.x
18. Kuang X.J., Xia H.T., Liao F.H., Wang C.H., Li L., Jing X.P., Tang Z.X. (2007): Doping effects of Ta on conductivity and microwave dielectric loss of $MgTiO_3$ ceramics. *Journal of the American Ceramic Society*, *90*, 3142-3147. doi:10.1111/j.1551-2916.2007.01899.x
19. Templeton A., Wang X.R., Penn S.J., Webb S.J., Cohen L.F., Alford N.M. (2000). Microwave dielectric loss of titanium oxide. *Journal of the American Ceramic Society*, *83*, 95-100. doi:10.1111/j.1151-2916.2000.tb01154.x
20. https://en.wikipedia.org/wiki/Relative_permittivity.
21. Chen H., Tang B., Gao A., Duan S., Yang H., Li, Y.X., Li H., Zhang S.R. (2015): Aluminum substitution for titanium in $Ba_{3.75}Nd_{9.5}Ti_{18}O_{54}$ microwave dielectric ceramics. *Journal of Materials Science: Materials in Electronics*, *26*(1), 405-410. doi:10.1007/s10854-014-2414-0